



1 **Investigation of the relationship between drinking water quality and landform classes**
2 **using fuzzy AHP(case study: south of Firozabad, east of Fars province, Iran)**

3

4 **Marzieh Mokarram¹ and Dinesh Sathyamoorthy²**

5 ¹*Marzieh Mokarram(Department of Range and Watershed Management, College of Agriculture and*
6 *Natural Resources of Darab, Shiraz University, Iran, Email: m.mokarram@shirazu.ac.ir)*

7 ²*Dinesh Sathyamoorthy (Science & Technology Research Institute for Defence (STRIDE), Ministry of*
8 *Defence, Malaysia (E-mail: dinesh.sathyamoorthy@stride.gov.my)*

9 **Corresponding author:** *Marzieh Mokarram, Tel.: +98-917-8020115; Fax: +987153546476 , Address:*
10 *Darab, Shiraz university, Iran, Postal Code: 71946-84471, Email: m.mokarram@shirazu.ac.ir*



11 **Investigation of the relationship between drinking water quality and landform classes**
12 **using fuzzy AHP(case study: south of Firozabad, east of Fars province, Iran)**

13

14 **Abstract**

15 In this study, fuzzy analytic hierarchy process (AHP) is used to study the relationship between drinking
16 water quality and landform classes in south of Firozabad, east of Fars province, Iran. For determination
17 of drinking water quality, parameters of calcium (Ca), chlorine (Cl), magnesium (Mg), thorium (TH),
18 sodium (Na), electrical conductivity (EC), sulfate (So₄) and total dissolved solids (TDS) were used. It
19 was found that 8.29% of the study area have low water quality; 64.01%, moderate; 23.33%, high; and
20 very high, 4.38%. Areas with suitable drinking water quality are located in parts of the southeast and
21 southwest parts of the study area. The relationship between landform class and drinking water quality
22 show that drinking water quality is high in the stream, valleys, upland drainages and local ridge classes,
23 and low in the plain small and midslope classes.

24 **Keywords:** Drinking water quality, fuzzy AHP method, GIS, landform, south of Firozabad.

25

26 **1. Introduction**

27 Landform characteristics can affect the direction of water movement and water quality. Hence, in the
28 different landforms, there is different water quality (Bise, 2013). To this end, studies on the relationship
29 between landform classes and water quality have received significant attention. For example, William et
30 al. (2007) investigated runoff and water quality from three soil landform units on mancos shale. A survey
31 of sediment basins in steep, dissected shale up lands indicated that an average of 1.25 Mg/ha/year of
32 sediment is produced by that landform unit carefully designed and located basin plugs can be used
33 effectively to trap sediment, water, and salt from dissected shale uplands. Mehdi et al. (2012) determined
34 agricultural land use scenarios for modelling future water quality. The results showed that there is
35 relationship between types of land use and water quality. The impact of land use on water quality was
36 evaluated by Huang et al. (2013). The results indicated that there was significant negative correlation
37 between forest land and grassland and the water pollution, and the built-up area had negative impacts on
38 the water quality, while the influence of the cultivated land on the water quality was very complex.

39

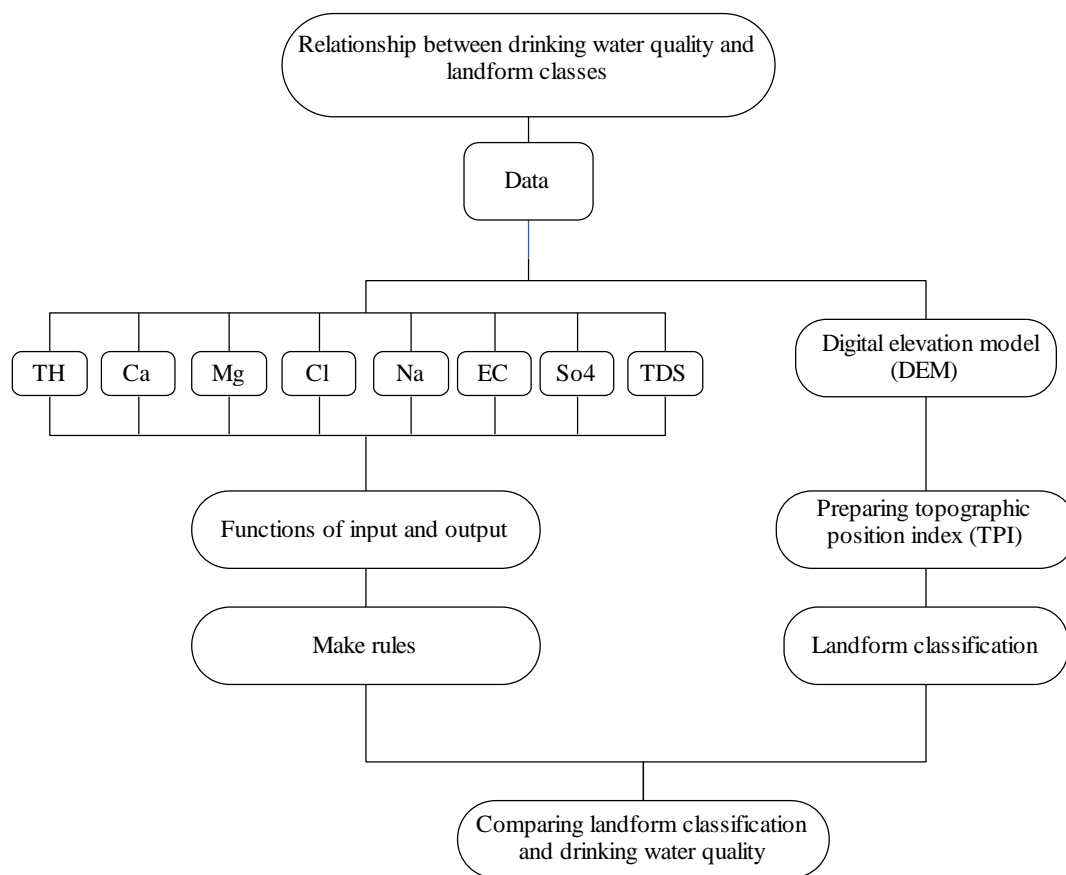


40 In addition, different algorithms have been employed for the determination of water quality. Yonas (2012)
41 developed a complementary modeling framework to handle systematic error in physically based
42 groundwater flow model applications that used data-driven models of the errors during the calibration
43 phase. The effectiveness of four error-correcting data-driven models, namely, artificial neural networks
44 (ANN), support vector machines (SVM), decision trees (DT) and instance based weighting (IBW) was
45 examined for forecasting head prediction errors, and subsequently updating the head predictions at
46 existing and proposed observation wells. Rule based modeling (Manoucher, 2010) was used for spatial
47 prediction of groundwater quality in Beaufort West, in the Karoo region of South Africa. The
48 groundwater quality data from about 100 bore wells with a 30 years span collected between 1970 and
49 2007 was used. The variables used in the analyses included chemicals such as chloride, sulphate,
50 magnesium, sodium, phosphates and calcium. These were used as predictors for groundwater quality and
51 electrical conductivity. Aliabadi and Soltanifard (2014) used fuzzy inference for determination of impact
52 of water and soil electrical conductivity and calcium carbonate on wheat crop using. The inference
53 system estimated the performance using soil EC, water EC and calcium carbonate in the soil as input
54 parameters, and also analyzed them.

55

56 The aim of this study is the determination of the relationship between landform classes and drinking
57 water quality in south Firozabad, Iran. In this study, drinking water quality is evaluated using
58 parameters of calcium (Ca), chlorine (Cl), magnesium (Mg), thorium (TH), sodium (Na), electrical
59 conductivity (EC), sulfate (So₄) and total dissolved solids (TDS). It is proposed that the most
60 appropriate method to prepare drinking water quality maps is fuzzy analytic hierarchy process (AHP)
61 in a geographic information system (GIS) environment. It is expected that the determination of the
62 relationship between landform classes and drinking water quality will allow for the prediction of
63 drinking water quality based on landform classes. The methodology employed in this study is
64 summarized in Figure 1.

65



66
 67 Figure 1. Flowchart for the methodology used in this study to determine the relationship between drinking
 68 water quality and landform classes.
 69

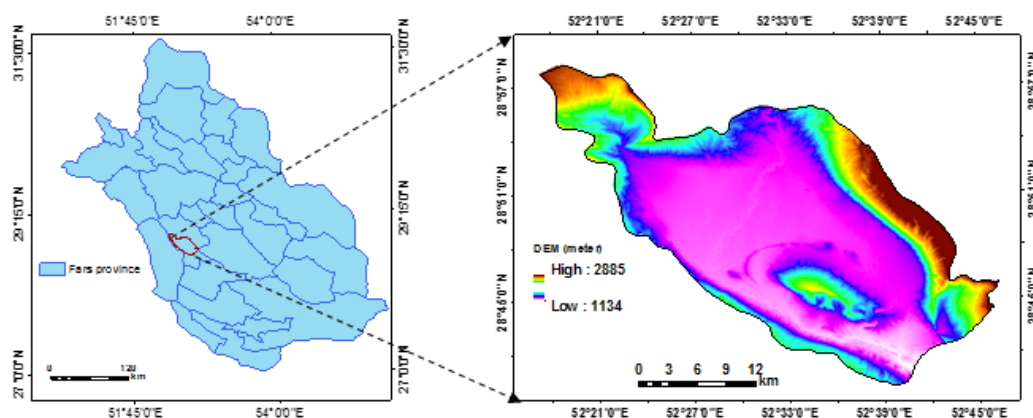
70 2. Material and method

71 2.1. Case study

72 This study was carried out in south of Firozabad, east of Fars Province, Iran. It has an area of 722.91 km²,
 73 and is located between longitude of N 28° 36' - 28° 57' and latitude of E 52° 16' to 52° 46' (Figure 2).
 74 The altitude of the study area ranges from the lowest of 1,134 m to the highest of 2,885 m. The study area
 75 is abundantly watered by springs and the perennial Firozabad river. The main agricultural produce
 76 consists of grain, fruit, and vegetables, while the partly wooded mountains are used for pasture (Ebn al-
 77 Balkr, 1912; Sharifi-Rad, 2014). The assessment of land suitability for agricultural production in the
 78 region is vital, which should consider environmental factors and human conditions.



79



80 Figure 2. Location of the study area (digital elevation model (DEM) with spatial resolution of 30 m)
 81 (Source: <http://earthexplorer.usgs.gov>).

82

83 One of these important factors is drinking water quality in the study area. In order to predict the
 84 variability of drinking water quality, calcium (Ca), chlorine (Cl), magnesium (Mg), thorium (TH),
 85 sodium (Na), electrical conductivity (EC), sulfate (So₄), total dissolved solids (TDS) were prepared
 86 (Table 1) (Fars Regional Water Authority).

87 Table 1. Descriptive statistics of the parameters for evaluation of water quality (Fars Regional Water
 88 Authority).

Parameters	Unit	Minimum	Maximum	mean	Stdv dev.
Calcium (Ca)	mg/l	0	596	195	89
Chlorine (Cl)	mg/l	25	437	84	45
Sodium (Na)	mg/l	0	458	51	45
Electrical, conductivity (EC)	ds/m	0.39	1.75	0.71	0.15
Magnesium (Mg)	mg/l	0	569	182	80
Sulfate (So ₄)	mg/l	0	584	137	73
Thorium (TH)	mg/l	0	473	180	77
Total Dissolved Solids (TDS)	mg/l	0	954	295	117

89



90 **2.2. Ordinary Kriging (OK)**

91 The input parameters for determination of drinking water quality are Ca, Cl, Mg, TH, Na, EC, So₄ and TDS.
 92 Interpolation maps of these parameters are prepared using ordinary kriging (OK). The presence of a spatial
 93 structure where observations close to each other are more alike than those that are far apart (spatial
 94 autocorrelation) is a prerequisite to the application of geostatistics (Goovaerts, 1999). The experimental
 95 variogram measures the average degree of dissimilarity between unsampled values and a nearby data
 96 value, and thus, can depict autocorrelation at various distances. The value of the experimental variogram
 97 for a separation distance of h (referred to as the lag) is half the average squared difference between the
 98 value at $z(x_i)$ and the value at $z(x_i + h)$: (Oliver, 1990):

99

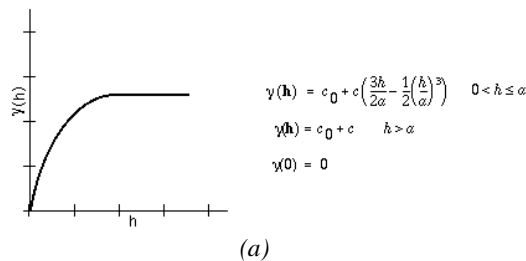
$$100 \quad \bar{\gamma}(h) = \frac{1}{2N(h)} \sum_{i=1}^{N(h)} [z(x_i) - z(x_i + h)]^2 \quad (1)$$

101

102 where N is the number of pairs of sample points $z(x_i)$ and $z(x_i + h)$ separated by distance h and $\bar{\gamma}(h)$ is the
 103 semivariogram. From the analysis of the experimental variogram, a suitable model is then fitted, usually
 104 by weighted least squares and four parameters; sill, range, nugget and anisotropy. Sill refers to the
 105 variance value at which the curve reaches the plateau sill. The total separation distance from the lowest
 106 variance to the sill is known as range. Semivariogram modeling is a key step between spatial description
 107 and spatial prediction. The main application of kriging is the prediction of attribute values at unsampled
 108 locations. There are several models for semivariogram graphs. Figure 3 shows the general shapes and
 109 equations of the mathematical models used to describe the semivariance (McBratney and Webster, 1986).

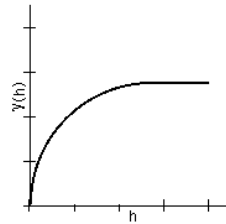
110

SPHERICAL





CIRCULAR



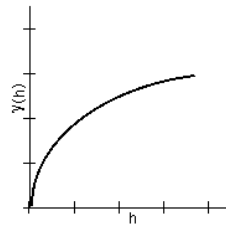
$$\gamma(h) = c_0 + c \left(1 - \frac{2}{\pi} \cos^{-1} \left(\frac{h}{\alpha} \right) + \sqrt{1 - \frac{h^2}{\alpha^2}} \right) \quad 0 < h \leq \alpha$$

$$\gamma(h) = c_0 + c \quad h > \alpha$$

$$\gamma(0) = 0$$

(b)

EXPONENTIAL

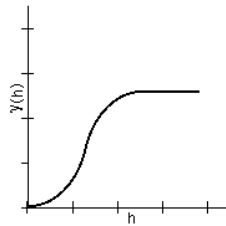


$$\gamma(h) = c_0 + c \left(1 - \exp\left(-\frac{h}{r}\right) \right) \quad h > 0$$

$$\gamma(0) = 0$$

(c)

GAUSSIAN



$$\gamma(h) = c_0 + c \left(1 - \exp\left(-\frac{h^2}{r^2}\right) \right) \quad h > 0$$

$$\gamma(0) = 0$$

(d)

111 Figure 3. Semivariogram graphs: (a) Spherical (b) Circular (c) Exponential (d) Gaussian

112

113 In order to compare, the different interpolation techniques, we examined the difference between known
 114 and predicted data using root mean squared error (RMSE) (Eq. (2))

115
$$\text{RMSE} = \sqrt{\frac{1}{N} \sum_{i=1}^N \{z(x_i) - \hat{z}(x_i)\}^2}$$
 (2)

116

117 where $\hat{z}(x_i)$ is the predicted value, $z(x_i)$ is the observed (known) value, and N is the number of values in
 118 the dataset (Johnston et al., 2001).

119



147

148

Table 2. Drinking water quality standards (WHO) (Shobha et al., 2013)

Parameters	Permissible limit (mg/liter)
Calcium (Ca)	200
Chlorine (Cl)	200
Magnesium (Mg)	150
Thorium (TH)	500
Sodium (Na)	200
Electrical conductivity (EC)	3000
Sulfate (So ₄)	200
Total Dissolved Solids (TDS)	500

149 **Analytic hierarchy process (AHP)**

150 AHP is a structured technique for organizing and analyzing complex decisions. This method is based on a
 151 pair-wise comparison matrix. The matrix is called consistent if the transitivity (Equation (6)) and
 152 reciprocity (Equation (7)) rules are respected:

153

154 $a_{ij} = a_{ik} \cdot a_{kj}$ (6)

155 $a_{ij} = 1/a_{ji}$ (7)

156

157 where i, j and k are any alternatives of the matrix.

158

159 In a consistent matrix (Equation (8)), all the comparisons a_{ij} obey the equality $a_{ij} = p_i/p_j$, where p_i is the
 160 priority of the alternative i . When the matrix contains inconsistencies, two approaches can be applied:

161
$$\begin{pmatrix} P_1/P_1 & \dots & P_1/P_j & \dots & P_1/P_n \\ \dots & 1 & \dots & \dots & \dots \\ P_i/P_1 & \dots & 1 & \dots & P_i/P_n \\ \dots & \dots & \dots & 1 & \dots \\ P_n/P_1 & \dots & P_n/P_j & \dots & P_n/P_n \end{pmatrix}$$
 (8)

162 In this method, pair-wise comparisons are considered as input, while relative weights are considered as
 163 outputs. The average of each row of the pair-wise comparison matrix is calculated and these average
 164 values indicate relative weights of compared criteria.



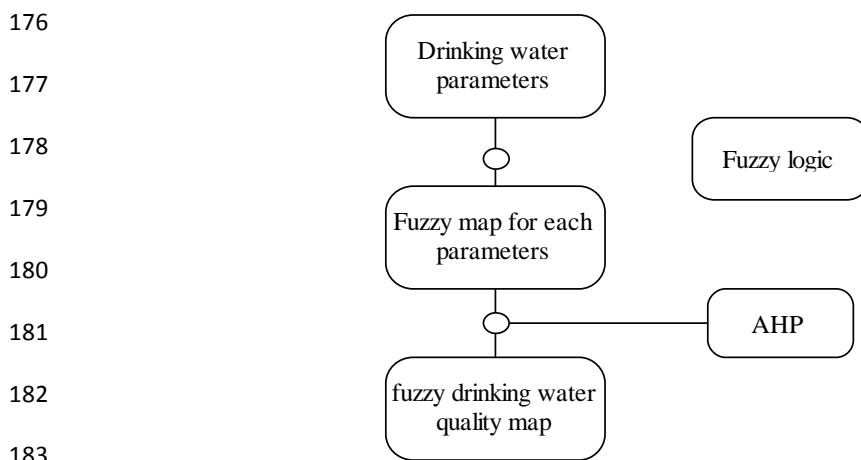
165 **Combination of fuzzy and AHP methods**

166 Finally, in order to prepare the drinking water quality map, it is necessary to calculate the convex
 167 combination of the raster values containing the different fuzzy parameters. A_1, \dots, A_k are fuzzy subclasses
 168 of the defined universe of objects X , and W_1, \dots, W_k are non-negative weights summing up to unity. The
 169 convex combination of A_1, \dots, A_k is a fuzzy class A (Burrough, 1989), and the weights W_1, \dots, W_k are
 170 calculated using AHP and fuzzy method parameters that have been calculated in ArcGIS. Equations 9 and
 171 10 show the convex combination.

172
$$\mu_A = \sum_{j=1}^k W_j \times \mu_{A(x)} \quad x \in X \quad (9)$$

173
$$\sum_{j=1}^k W_j = 1 \quad W_j > 0 \quad (10)$$

174 The Fuzzy AHP approach in this study has been divided into five stages, which are summarized in Figure
 175 4.



184 Figure 4. Fuzzy AHP procedure for drinking water quality.

185

186 All the model parameters maps are constructed by interpolation between 50 sampling points using the
 187 kriging method. Next, fuzzy logic is applied to create a fuzzy parameter map for each parameter. To
 188 arrive at an integrated evaluation using drinking water quality classes, the fuzzy parameter maps were
 189 aggregated into a drinking water quality map following a weighted summation using AHP.

190



191

192 **2.4. Landform Classification Using Topographic Position Index (TPI)**

193 TPI (Weiss, 2006) compares the elevation of each cell in a DEM to the mean elevation of a specified
 194 neighborhood around that cell. Positive and negative TPI values represent locations that are higher and lower
 195 than the average of their surroundings respectively. TPI values near zero are either flat areas (where the slope
 196 is near zero) or areas of constant slope (where the slope of the point is significantly greater than zero) (Weiss
 197 2006).

198 TPI (Eq. (11)) compares the elevation of each cell in a DEM to the mean elevation of a specified
 199 neighborhood around that cell. Mean elevation is subtracted from the elevation value at the center (Weiss
 200 2006):

$$201 \quad TPI_i = T_0 - \frac{\sum_{n=1}^{n-1} T_n}{n} \quad (11)$$

202 where;

203 T_0 = elevation of the model point under evaluation

204 T_n = elevation of grid

205 n = the total number of surrounding points employed in the evaluation.

206

207 Combining TPI at small and large scales allows a variety of nested landforms to be distinguished Table 3.

208

209

Table 3. Landform classification based on TPI ,(Source: Weiss 2006)

Classes	Description
Canyons, deeply incised streams	Small Neighborhood: $T_o \leq -1$
	Large Neighborhood: $T_o \leq -1$
Midslope drainages, shallow valleys	Small Neighborhood: $T_o \leq -1$
	Large Neighborhood: $-1 < T_o < 1$
upland drainages, headwaters	Small Neighborhood: $T_o \leq -1$
	Large Neighborhood: $T_o \geq 1$
U-shaped valleys	Small Neighborhood: $-1 < T_o < 1$
	Large Neighborhood: $T_o \leq -1$
Plains small	Neighborhood: $-1 < T_o < 1$
	Large Neighborhood: $-1 < T_o < 1$
	Slope $\leq 5^\circ$
Open slopes	Small Neighborhood: $-1 < T_o < 1$
	Large Neighborhood: $-1 < T_o < 1$



	Slope > 5°
Upper slopes, mesas	Small Neighborhood: $-1 < T_o < 1$ Large Neighborhood: $T_o \geq 1$
Local ridges/hills in valleys	Small Neighborhood: $T_o \geq 1$ Large Neighborhood: $T_o \leq -1$
Midslope ridges, small hills in plains	Small Neighborhood: $T_o \geq 1$ Large Neighborhood: $-1 < T_o < 1$
Mountain tops, high ridges	Small Neighborhood: $T_o \geq 1$ Large Neighborhood: $T_o \geq 1$

210

211 **4. Results and Discussion**

212 **4.1. Geostatistical analysis**

213 OK was used for the prediction of the drinking water quality parameters (TH, Ca, Mg, Cl, Na, EC, So4
 214 and TDS). In OK, in order to select the best method (Circular, Spherical, Exponential and Gaussian),
 215 measured nugget, partial sill and RMSE were used (Table 4). The RMSE of water parameters from Table
 216 4 shows that the lowest RMSE is the Gaussian method. Furthermore, these results indicate that the
 217 Gaussian model for OK is the best semivariogram model to show the strong spatial dependency for the
 218 water variable.

219 Table 4. Sampling nugget, partial sill and RMSE of the different interpolated methods for predicted
 220 drinking water quality using MLR.

Methods	Model	Parameter	Nugget	Partial Sill	RMSE
OK	Circular	TDS	0.66	0.32	0.80
		TH	0.7	0.229	0.80
		Ca	0.71	0.20	0.92
		Mg	0.70	0.36	0.61
		Na	0.63	0.45	0.90
		Cl	0.57	0.38	0.77
		So4	0.62	0.29	0.91
		EC	0.57	0.26	0.56
	Spherical	Parameter	Nugget	Partial Sill	RMSE
		TDS	0.67	0.32	0.80
		TH	0.69	0.30	0.81
		Ca	0.72	0.20	0.92
		Mg	0.70	0.37	0.61
		Na	0.63	0.44	0.90
Cl	0.57	0.37	0.77		
So4	0.62	0.30	0.91		
EC	0.55	0.28	0.56		
	Parameter	Nugget	Partial Sill	RMSE	

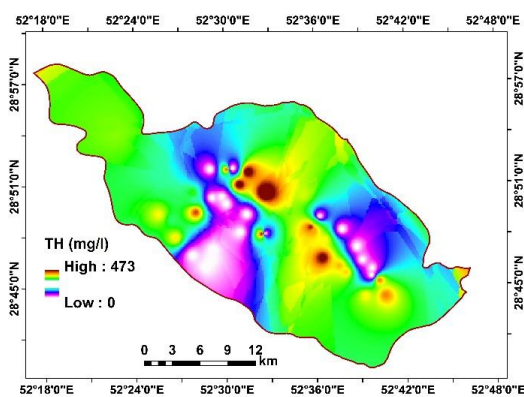


Exponential	TDS	0.62	0.32	0.81
	TH	0.63	0.37	0.82
	Ca	0.70	0.20	0.93
	Mg	0.69	0.36	0.62
	Na	0.63	0.45	0.91
	Cl	0.55	0.35	0.78
	So4	0.56	0.36	0.92
	EC	0.44	0.39	0.62
Gaussian	Parameter	Nugget	Partial Sill	RMSE
	TDS	0.67	0.32	0.79
	TH	0.73	0.27	0.80
	Ca	0.71	0.21	0.91
	Mg	0.71	0.36	0.60
	Na	0.64	0.45	0.90
	Cl	0.57	0.39	0.76
	So4	0.66	0.26	0.89
EC	0.57	0.26	0.53	

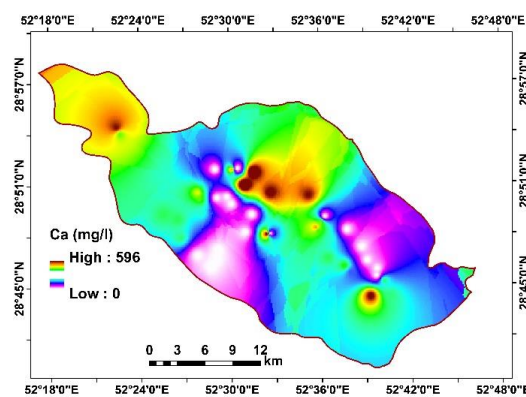
221

222 Each of water parameters map that was predicted by OK is shown in Figure 5. The lowest So4, TDS, Na,
 223 Mg, TH and Ca were 0, while the highest values for the parameters were 589, 954, 458, 569, 473 and 569
 224 mg/l respectively. The lowest values for EC and Cl were 0.39 and 25 mg/l respectively, while the highest
 225 were 1.7 and 437 respectively. In the total, the results showed that expect for Ca and Mg, the other
 226 parameters had high values in the study area.

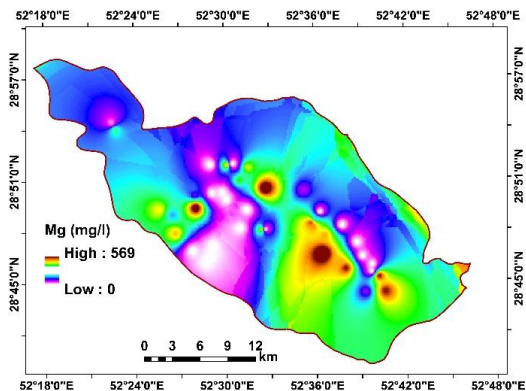
227



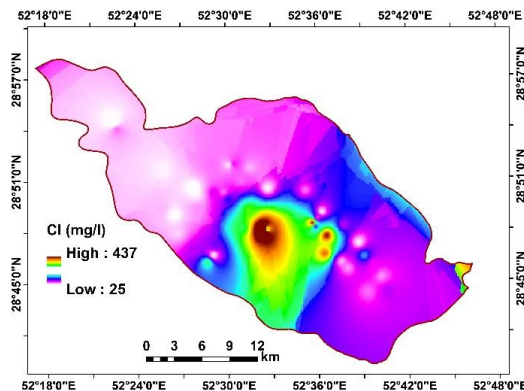
TH



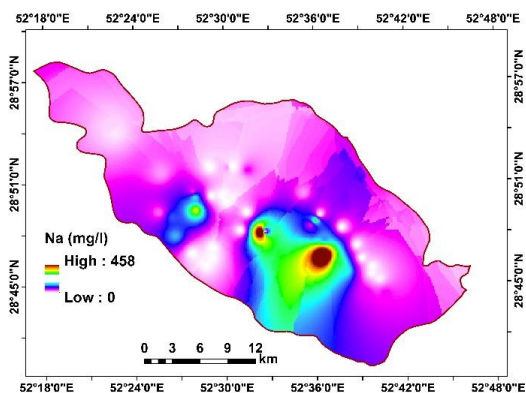
Ca



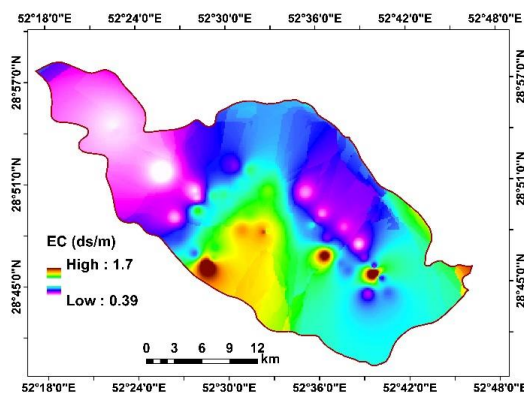
Mg



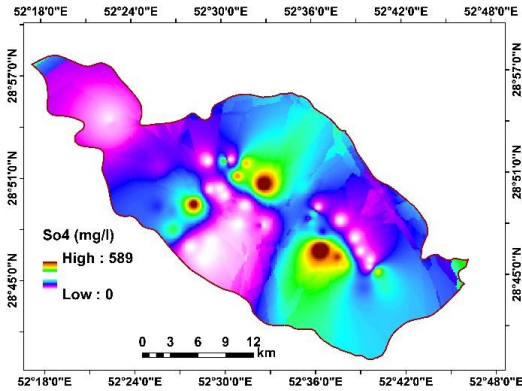
Cl



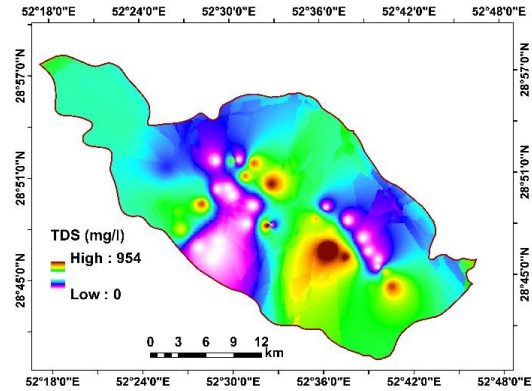
Na



EC



So₄



TDS

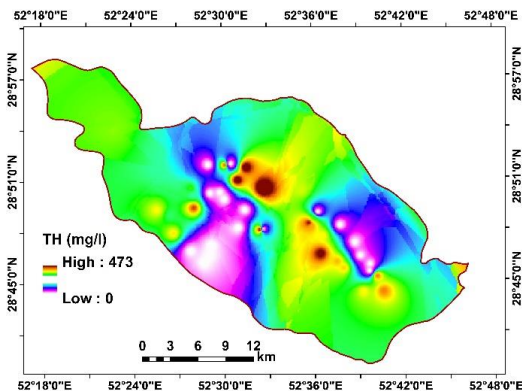
228 Figure 5. Interpolated maps of the drinking water quality parameters generated using by OK.

229

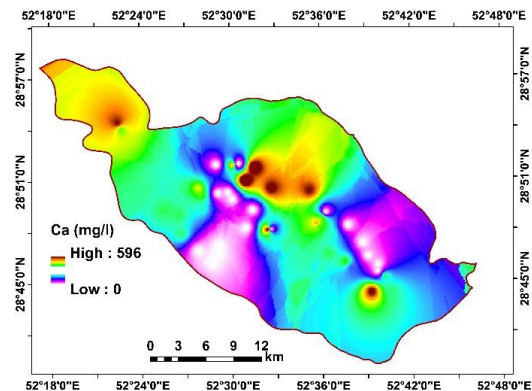
230 4.2. Fuzzy method

231 The fuzzy maps prepared for the drinking water quality parameters are shown in Figure 6, where MF is
232 closer to 0 with decreasing drinking water quality, while MF is closer to 1 with increasing drinking water
233 quality (Soroush et al., 2011). Next, the AHP method was applied on the fuzzy parameter maps. The
234 pair-wise comparison matrix used for preparation of the weights for each parameter in AHP are given in
235 Table 5. The drinking water quality map generated using fuzzy-AHP is shown in Figure 7.

236



TH



Ca

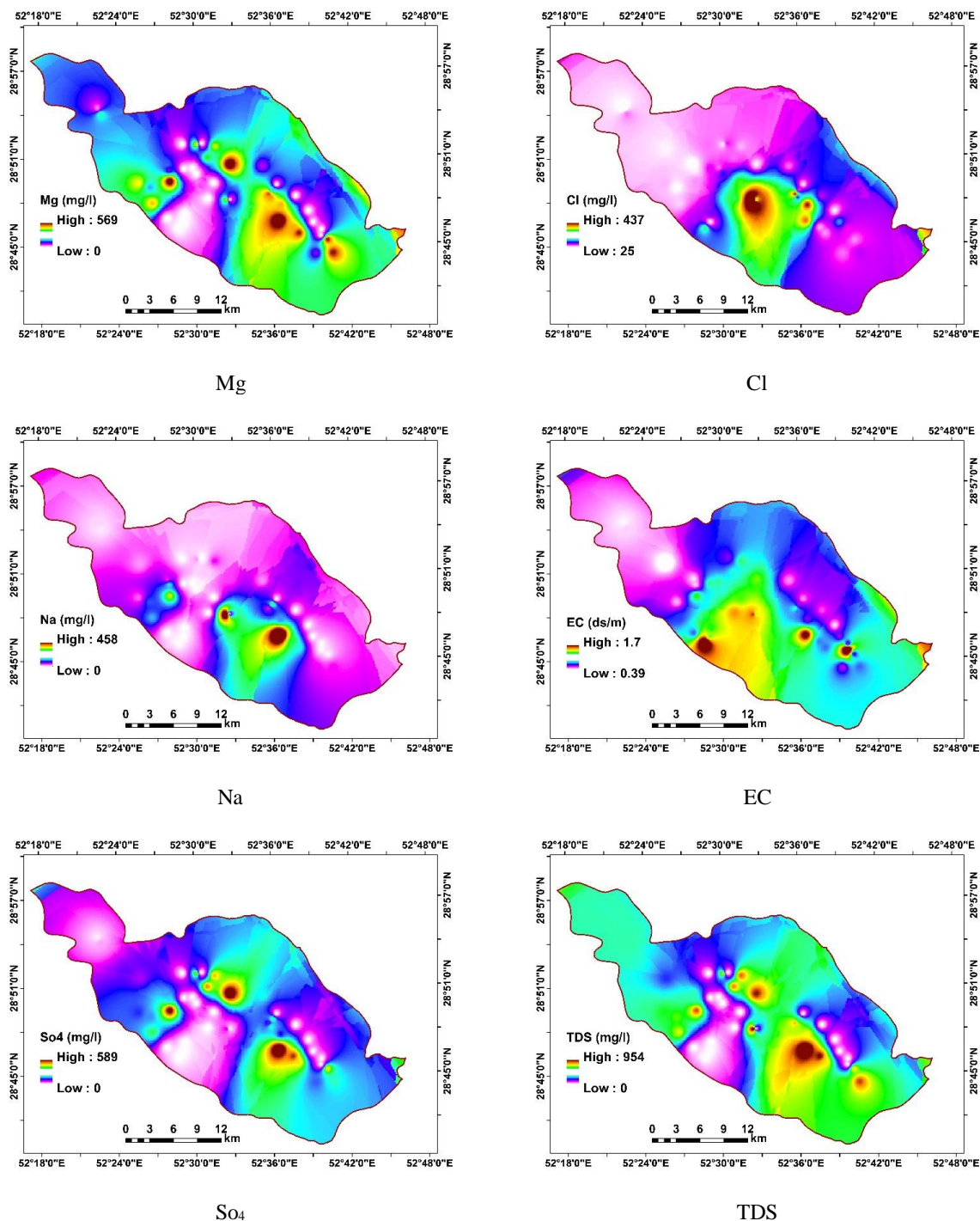


Figure 6. Fuzzy maps of study area for the drinking water quality parameters.

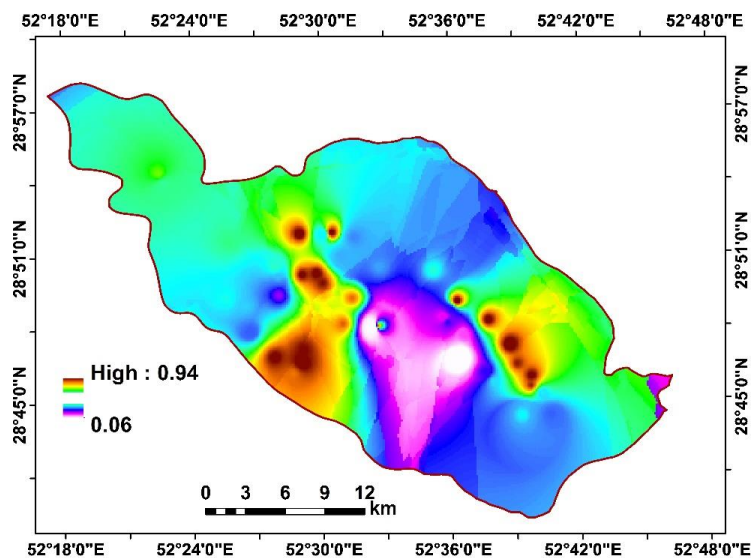


238

Table 5. Pair-wise comparison matrix for drinking water quality.

parameters	Ca	Cl	Na	EC	Mg	So4	TH	TDS	Weight
Ca	1	2	3	4	5	6	7	8	0.33
Cl	0.5	1	2	3	4	5	6	7	0.23
Na	0.33	0.5	1	2	3	4	5	6	0.16
EC	0.25	0.33	0.5	1	2	3	4	5	0.11
Mg	0.2	0.2	0.33	0.5	1	2	3	4	0.07
So4	0.16	0.16	0.2	0.33	0.5	1	2	3	0.05
TH	0.14	0.14	0.16	0.2	0.33	0.5	1	2	0.03
TDS	0.12	0.12	0.14	0.16	0.2	0.33	0.5	1	0.02

239



240

241 Figure 7. Drinking water quality map generated using fuzzy AHP.

242

243



244

245 The drinking water quality map is classified into four classes (Mokarram et al., 2010; Shobha et al.,
246 2013):

- 247 ➤ Low (not suitable for drinking): < 0.25
- 248 ➤ Moderate: $0.25 - 0.50$
- 249 ➤ High: $0.50 - 0.75$
- 250 ➤ Very high (suitable for drinking): > 0.75

251

252 The results of the classification are shown in Table 6. It is found that areas with suitable drinking water
253 quality are located in the southeast and southwest parts of the study area (Figure 7).

254

255

Table 6. Areas of the drinking water classes.

Class	Area	
	(%)	(km ²)
Low	8.29	59.90
Moderate	64.01	462.72
High	23.33	168.65
Very high	4.38	31.64

256

257

258

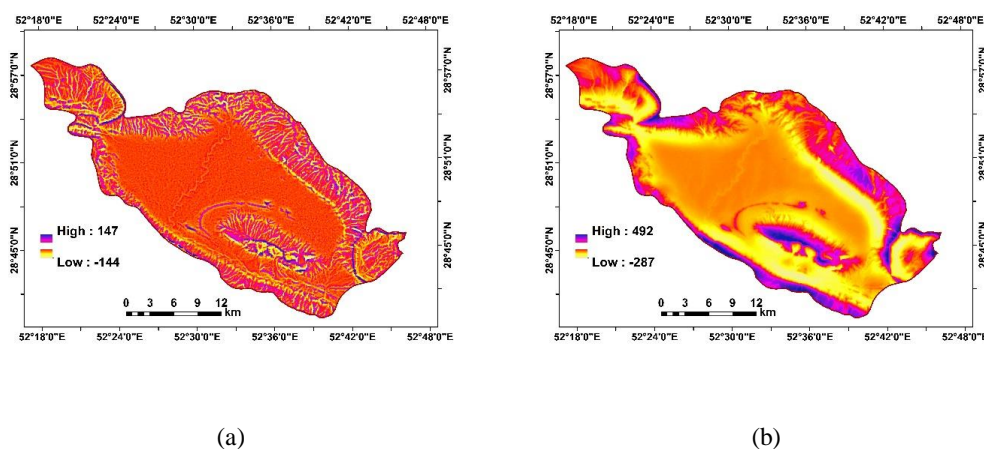
259 **4.3. Landform classification**

260 In order to determine the relationship between landform classification and drinking water quality, a
261 landform classification map for the study area was prepared using TPI. The TPI maps generated using
262 small (3 cells) and large (45 cells) neighborhoods are shown in Figure 8. TPI is between -144 to 147 and -
263 287 to 492 for the small and large neighborhoods respectively. The landform maps generated based on the
264 TPI values are shown in Figure 10. The classification has ten classes; high ridges, midslope ridges, upland
265 drainage, upper slopes, open slopes, plains, valleys, local ridges, midslope drainage and streams (Figure
266 9). The areas of the landform classes are shown in Figure 10. It is observed that the largest landform is
267 streams, while the smallest is plains.

268

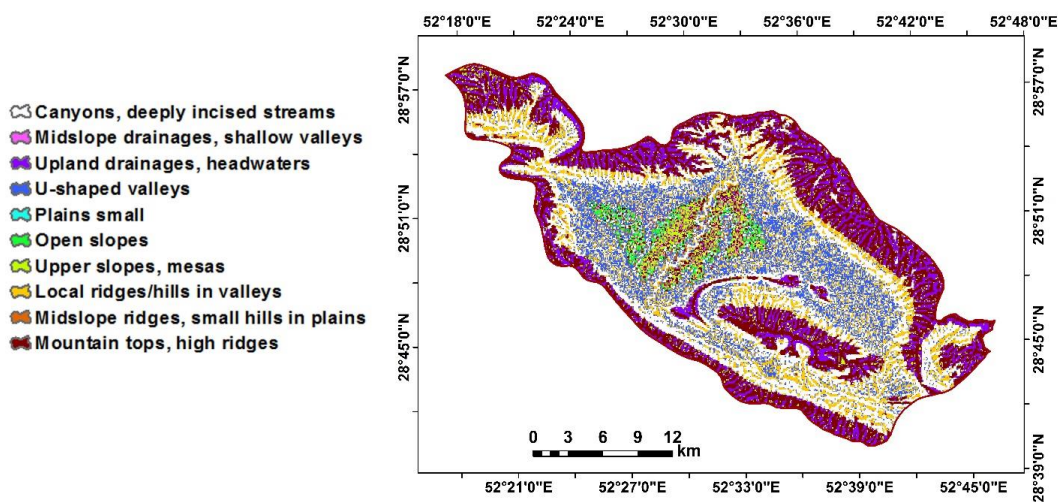
269

270



271
 272
 273
 274

Figure 8. TPI maps generated using (a) small (3 cells) and (b) large (45 cells) neighborhoods.

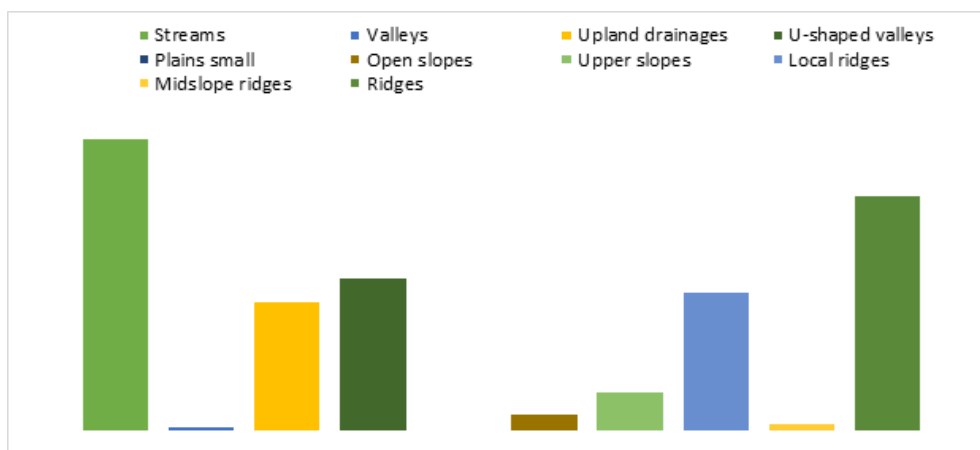


275
 276

Figure 9. Landform classification using the TPI method.



277



278

Figure 10. Areas of the landform classes.

279

280 The relationship between drinking water quality and landform classes were determined (Figure 11). It is
281 found that drinking water quality is high for streams, valleys, upland drainages and local ridge classes,
282 while the lowest drinking water quality is in the plain small and midslope classes. The characteristics of
283 landform classes, such as slope and geology, determine the drinking water quality. For example, in the
284 plain small class, due to the low slope, there are ample opportunities for high drinking water quality
285 (Christiansen, 2004). Therefore, landform maps can be used to predict drinking water quality without
286 water sampling and analysis in the laboratory.

287



288

289

290

291

292

293

294

295

296

297

298



299

Figure 11. Relationship between drinking water quality and landform classes.

300

301

302 5. Conclusions

303 In this study, fuzzy AHP was used to study the relationship between drinking water quality and landform
304 classes in south of Firozabad. It was found that 8.29% of the study area had low water quality; 64.01%,
305 moderate; 23.33%, high; and 4.38%, very high. The lands suitable for drinking water are located in the
306 southeast and southwest parts of the study area. The relationship between landform class and drinking
307 water quality show that drinking water quality is high in the stream, valleys, upland drainages and local
308 ridge classes, while the lowest drinking water quality is in the plain small and midslope classes.

309

310

311 Reference

- 312 1. Aliabadi, K., Soltanifard, H. 2014. The Impact Of Water And Soil Electrical Conductivity And
313 Calcium Carbonate On Wheat Crop Using A Combination Of Fuzzy Inference System And GIS.
314 International Journal of Scientific & Technology Research. Vol.3, No.9.



- 315 2. Badenko, v., and kurtener, D. 2004. Fuzzy modeling in GIS environment to support sustainable
316 land use planning. The AGILE conference on geographic information science.29 April-1may.
317 Heralion, Greece, parallel session a.1-geographic knowledge discovery.
- 318 3. Bise, C J. 2013. Modern American Coal Mining: Methods and Applications. Society for Mining
319 Metallurgy & Exploration. ISBN: 9780873353526.
- 320 4. Burrough, P.A. 1989. Fuzzy Mathematical Methods for Soil Survey and Land Suitability. Journal
321 of Soil Science 40: 477-492.
- 322 5. Demissie, Y., Yan, E., and Wu, M., 2012. Assessing Regional Hydrology and Water Quality
323 Implications of Large-Scale Biofuel Feedstock Production in the Upper Mississippi River Basin,
324 Environmental Science & Technology, DOI: 10.1021/es300769k.
- 325 6. Ebn al-Balkr, Fars-nama, tr. G. Le Strange as Description of the Province of Fars, London, 1912.
326 7. Fars Regional Water Authority. <http://www.frrw.ir>.
- 327 8. Goovaerts, P. 1999. Geostatistics in Soil Science: State-of- the-Art and Perspectives, Geoderma,
328 Vol. 89, No. 1-2,1999, pp. 1-45.
- 329 9. Huang, J., Zhan, J., Yan, H., Wu, F., Deng, X. 2013. Evaluation of the Impacts of Land Use on
330 Water Quality: a case study in the Chaohu lake basin. The Scientific World Journal.
331 Volume 2013, Article ID 329187, 7 pages.
- 332 10. Johnston, K., Hoef, J. M. V., Krivoruchko K., Lucas, N. Using ArcGISTM Geostatistical
333 Analyst, ESRI. 380, New York, 2001.
- 334 11. Kurtener D, Green TR, Krueger–Shvetsova E, Erskine RH. 2005, Exploring Relationships
335 Between Geomorphic Factors and Weaht Yield Using Fuzzing Inference System, Hydrology
336 Days, 121-130
- 337 12. Manoucher A, Mini karim C, Annette John, A comparison on a different rule based statistical
338 models for modeling geogenic groundwater contamination, Journal of Environmental modeling
339 & Software, Vol 25, Issue 12, December 2010, pp. 1650-1657.
- 340 13. Mc Bratney, A.B., Odeh, I.O.A. 1997. Application of Fuzzy sets in soil science: Fuzzy logic.
341 Fuzzy measurements and Fuzzy decisions, Geoderma 77: 85-113.
- 342 14. McBratney, A. B., and R. Webster. 1986. Choosing Functions for Semi-variograms of Soil
343 Properties and Fitting Them to Sampling Estimates. Journal of Soil Science 37: 617–639.
- 344 15. Mehdi, B.B., Ludwig, R., Lehner, B. 2012. Determining agricultural land use scenarios in a
345 mesoscale Bavarian watershed for modelling future water quality. Advances in Geosciences
346 (ADGEO). 31, 9–14.



- 347 16. Mokarram, M., Rangzan, K., Moezzi, A., Baninemehc, J. 2010. Land suitability evaluation for
348 wheat cultivation by fuzzy theory approache as compared with parametric method. The
349 international archives of the photogrametry, Remote sensing and spatial information sciences,
350 Vol. 38, part II, pp 1440-145.
- 351 17. Oliver, M. A. 1990. Kriging: A Method of Interpolation for Geographical Information Systems.
352 International Journal of Geographic Information Systems 4: 313–332. 1990.
- 353 18. Sharifi-Rad J., Hoseini-Alfatemi, S.M., Sharifi-Rad M., Setzer, W.N. 2014. Chemical
354 composition, antifungal and antibacterialActivities of essential oil from lallemantia Royleana
355 (benth. In wall.) Benth. Journal of Food Safety 35 (2015) 19–25 © 2014 Wiley Periodicals, Inc.
- 356 19. Shobha, G., Gubbi, J., Raghavan, K.S., Kaushik, K., Palaniswami. M. 2013. A novel fuzzy rule
357 based system for assessment of ground water potability: A case study in South India. IOSR
358 Journal of Computer Engineering (IOSR-JCE). Volume 15, Issue 2 (Nov. - Dec. 2013), PP 35-41
- 359 20. Soroush, F., Mousavi, S. F., Gharechahi A. 2013. A fuzzy industrial water quality index: case
360 study of zayandehrud river system. IJST, Transactions of Civil and Environmental Engineering,
361 Vol. 35, No. C1, pp 131-136
- 362 21. Weiss, A. (2006). Topographic Position and landforms Analysis. Poster presentation, ESRI
363 userConference, San Diego, C.A.
- 364 22. William L. Jackson and Randall P. Julande. 2007. Runoff and water quality from three soil
365 landform units on mancos shale. JAWRA Journal of the American Water Resources Association.
366 Volume 18, Issue 6, pages 995–1001,
- 367 23. Zadeh, L.H. 1965. Fuzzy sets. Information and Control 8: 338–353.